



Design, Fabrication and Optimization of an Automated Groundnut Shelling Machine

ABIRHIRE, O. E.¹ , MARKSON, I. E.² , ANAIDHUNO, U. P.³ , ASHIEDU, F. I.⁴

^{1,3,4}Department of Mechanical Engineering, Federal University of Petroleum Resources, Effurun, Nigeria

²Department of Mechanical and Aerospace Engineering, University of Uyo, Uyo, Nigeria

ARTICLE INFO

Received: 13/04/2025

Accepted: 22/07/2025

Keywords

Automated, Design,
Fabrication,
Groundnut, Machine,
Shelling

ABSTRACT

This research investigated the design, fabrication and optimization of an automated groundnut shelling machine to overcome challenges associated with manual shelling, including increased labour costs, longer processing times, and inconsistent shelling quality. The methodology involves a multi-objective optimization approach, considering factors such as the radius of the shelling drum, radius of the concave mesh, surface area in contact with shelling blades, rasp bar spacing, and the number of shelling blades. The performance evaluation includes mechanical damage, shelling efficiency, and throughput capacity, measured through experiments using groundnut seeds. Material selection for the groundnut sheller was based on a materials index. The result showed that carbon steel is the most preferable material, followed by low alloy steel, aluminium, wrought iron, stainless steel, and oak wood. A global optimal condition was found at radius of the shelling drum (X1) of 0.17, radius of the concave mesh (X2) of 0.0914, surface area in contact with shelling blades (X3) of 0.424, rasp bar spacing (X4) of 0.013 and number of shelling blades (X5) of 3. At these conditions, mechanical damage (Y1), shelling efficiency (Y2), and throughput capacity (Y3) were 12.32%, 80.4942% and 50.22 g/sec respectively. The validation of the mathematical model through ANOVA confirms the adequacy and significance of the coefficients in the developed model. The Pareto chart visually represents the standardized effects of different parameters, providing insights into the relative importance of factor combinations. The designed and fabricated machine demonstrated promising results and reduced damage.

1. INTRODUCTION

Groundnut, also known as peanut, is an important crop cultivated worldwide for its nutritional value and economic significance. It serves as a source of protein, oil, and essential nutrients for human consumption and is used in various food products. However, the traditional manual shelling process for groundnut is labour-intensive, time-consuming, and inefficient. This poses challenges for farmers and

processors, leading to reduced productivity, increased labour costs, and post-harvest losses. Therefore, the automated machine for the shelling process is essential to improve efficiency, increase productivity, and economic viability of groundnut cultivation and processing.

The sixth-most significant oilseed crop in the world is groundnut. Rich in nutritional fibre, minerals, and vitamins, it has a 46–50% oil content and a 25–28% protein

*Corresponding author, e-mail: engrkekule02@gmail.com, idorenyinmarkson@uniuyo.edu.ng, anaidhuno.ufuoma@fupre.edu.ng, ashiedu.ifeanyi@fupre.edu.ng

content. It thrives in loosely textured, well-drained soils that are also rich in calcium, potassium, and phosphorus, Ravindra et al. (2017). Grown in more than 100 countries globally, groundnuts. As per the FAOSTAT, United Nations in 2018 the world production of groundnut was 44 million tonnes, which lead by China with 38% of the global total followed by India 16%. Other significant producers were Nigeria, the United States, and Sudan. The production in millions of tonnes as follow China 16.6, India 6.9, Nigeria 3.0, United States 2.6, Sudan 1.8, and rest of world 44.0, Meneby et al. (2022). Given that groundnuts edible nutritious agricultural product, though India is at second position of producing groundnut in world, but still in developing countries like India, farmers take groundnut production in small scale.

Workers separated groundnuts or peanuts in various groundnut processing industries or at local businesses in the beginning. The output from this method was very less and could not satisfy the market demand as it was very time-consuming process, Chang et al. (2013). The study was to design and manufacture a simple groundnut shelling machine. The design is very simple and eco-friendly which uses simple mechanism properties such as shelling system, automatic separating system and crushing chamber etc. In this research work piece, separated machine parts, investigated forces and safety factor for people. This research provided a novel idea for groundnut shells (crush), which would be more portable and appropriate for groundnut crushing. Following completion, the design was turned into the actual product, where it serves as a reference. Nevertheless, Gupta et al. (2020) have created a basic groundnut shelling machine

that is handled by hand and has a closed, semi-cylindrical shape on both sides. The main disadvantage of this machine is that it requires a lot of labour and takes a long time

The machine addressed the labour-intensive nature of manual shelling, ensure consistent and high-quality shelling outcomes, reduce processing time, and provide a safe working environment for operators.

Hoque et al. (2013) undertook the design and development of a power groundnut sheller at the Farm Machinery and Postharvest Process Engineering (FMPE) Division of the Bangladesh Agricultural Research Institute (BARI) in Gazipur from 2011 to 2013. It was discovered that the power groundnut sheller had a 99% winnowing efficiency. When using the power groundnut sheller instead of manual techniques, shelling costs may be lowered by 76%. Consequently, for groundnut shelling in Bangladesh's small-scale industry and agricultural settings, the power groundnut sheller is advised.

Igbal et al. (2013) developed a groundnut shelling machine with the aim of improving kernel production. The stator held the groundnut in place while the roller rotated to mechanically break the pods. The machine's performance was assessed by varying the rotation speed of the motor, specifically SR 1, SR 2, and SR 3. Through one-way ANOVA analysis, it was determined that SR 1 demonstrated the fastest average operation (115.46 kg/h) with significant statistical difference ($p < 0.0001$). SR 2 and SR 3 followed with operation speeds of 96.78 kg/h and 99.89 kg/h, respectively. SR 1 also exhibited the lowest kernel damage at approximately 30.96% compared to the other rotations (p

<0.05). Additionally, the machine achieved over 99% shelling efficiency and less than 0.5% losses.

Mohammad et al. (2019) modified a locally created groundnut sheller. The shelling unit of the modified sheller comprises of a cleaning unit, a primary mover, a shelling chamber with a rasp bar, and a hopper with feed control. The improved sheller demonstrated an output capacity of 239.81 kg/h, a cleaning efficiency of 50.63%, a mechanical damage of 4.33%, a scatter loss of 3.24%, and a shelling efficiency of 98.32%. By contrast, the previous sheller's data showed an output capacity of 233.18 kg/h, an 86.19% shelling efficiency, an 8.11% cleaning efficiency, and a 9.52% scatter loss.

A peanut shelling machine that mimicked the manual peanut peeling process was created by Sun et al. (2017). A frame, a feeding mechanism, a pneumatic gripper, and a peanut shelling positioning mechanism make up the mechanical framework of the peanut shelling machine. A MCU, an LCD 12864 liquid-crystal display, and keys make up the control system. According to experimental findings, 92.3% of peanuts are successfully shelled at a rate of 20/min. Additionally, it offered a fresh method for achieving mechanized peanut shelling and productive agriculture.

Wangette et al. (2015) looked into how machine and groundnut properties affected the functionality of motorized shellers, in their observation, motorized Sheller's have different levels of kernel damage and shelling efficiencies that are less than 100%. The study discovered that when the moisture content (mc) dropped, the throughput per unit power consumption and

shelling efficiency rose, with the best outcomes occurring at 6% mc.

Adetola et al. (2022) conducted a comprehensive study on a groundnut shelling machine. The machine underwent three rounds of testing, with measured parameters including shelling efficiency (97.94%), cleaning efficiency (56.2%), material efficiency (90.13%), shelling capacity (192.86 kg/hr.), mechanical damage (9.87%), and estimated to be (\$330 USD). The results demonstrated the machine's efficient performance, suggesting its potential benefits in the industry in streamlining shelling operations. Galea et al. (2020); Gauthier et al. (2021) provide guidelines and insights into safety considerations in machinery design, Colim et al. (2021); Cardeso et al. (2021) guide the addition of ergonomic factors. The multi-objective optimization process involved decisions-based trade-offs Heua et al (2021). The software facilitates a systematic approach to performance evaluation by considering real-world mechanical damage, shelling efficiency, and throughput capacity, Sharifi et al. (2021). Changes in weights or priorities assigned to different objectives can impact the overall performance, Yazdani et al. (2016). A sensitivity analysis, as recommended by Sasikumar et al. (2023), helps in assessing the stability and reliability of the material selections.

There is a notable gap from studies on optimization. There is research also focused on the multi-objective method for shelling chamber optimization.

2. METHODOLOGY

2.1 Material selection

In designing the groundnut sheller, the materials and functions, shape and process,

were established. The current material selection aims to provide a groundnut sheller that is affordable, lightweight, and has better safety. Since the structural components used are essentially expected to perform physical tasks (carry load), they must meet functional specifications set forth by the design, including the specified tensile, deflection, and torsional load, etc. Therefore, a collection of material characteristics that describe a material's performance in the current groundnut sheller application constitutes the material performance index. Ashby et al. (2013), a structural element's performance may be determined by the functional requirements, the shape, and the material's characteristics, as shown in equation 1.

PERFORMANCE:

$$P \left[\begin{matrix} (Functional\ needs, F); \\ (Geometric, G); \\ (Material\ Property, M) \end{matrix} \right] \quad (1)$$

Therefore, we must either maximize or reduce the functional P for the best design. Consider only the simplest scenarios in which these variables may be separated by an equation, as in equation 2.

$$P = f_1(F)f_2(G)f_3(M) \quad (2)$$

If the specifics of factors F and G are known, Ashby et al., (2013) further asserted that the optimal subset of materials may be found using equation 2 without addressing the entire design issue. Consequently, by concentrating on the materials performance index $f_3(M)$, material performance may be improved. Detailed specification for the materials index are tabulated in Table 1

Table 1: Materials index used in selecting various shape/geometry machine element in groundnut sheller

S/N	Target	Stiffness relation	Mass	Materials performance index
1	lightweight, robust tension members	$\frac{\sigma_f}{S} = \frac{F}{c^2}$	ρLc^2	$\frac{\sigma_y}{\rho}$
2	Lightweight, rigid tension members	$\frac{F}{c^2} = E \frac{\delta}{L}$	ρLc^2	$\frac{E}{\rho}$
3	Light stiff beam under deflection loads	$\frac{F}{\delta} \geq \frac{C_1 EI}{L^3} = \frac{C_1 E}{L^3} \left(\frac{A^2}{12} \right)$	ρAL	$\frac{E^{1/2}}{\rho}$
4	Strong light torsional members	$\frac{\tau_f}{S} = \frac{2M_t}{\pi R^2}$	$\rho \pi L R^2$	$\frac{\tau_y^{2/3}}{\rho}$
5	Cheap stiff support for column	$F \leq F_{crit} = \frac{N\pi^2 EI}{L^2}$	$\rho AL C_m$	$\frac{E^{1/2}}{C_m \rho}$

Source: Adapted from Ashby et al., (2013), C_m = cost/mass, E = Elastic modulus, ρ = density, τ_y = shear stress, σ_y = fracture strength

2.2 Design Calculations

2.2.1 Power Required to Break the Groundnut Pods.

Considering a single spike, the torque required to drive the system may be obtained from the following expression:

$$T = n_a * n_s * F * r \quad (3)$$

Where,

n_a = number of active anchors at a time = 5

n_s = number of spikes per anchor = 7

F = force per spike required to break the groundnut pod

r = distance from the axis of rotation to point of action of the force = 0.11m

The average force required to break the groundnut pod is 2N. From equation (3), we get;

$$T = 5 \times 7 \times 2 \times 0.11 = 7.7 \text{ Nm}$$

The power required in breaking the pods in the shelling chamber may be obtained from;

$$P = T * \omega = T * \left(\frac{\pi * N}{30}\right) \quad (4)$$

From equation (4), we get

$$P = 7.7 * \left(\frac{\pi * 240}{30}\right) = 193.52 \text{ W}$$

2.3 Performance Optimization Variables

The methodology of multi-objective optimization involves the process of optimizing multiple conflicting objectives simultaneously.

The design factors and objectives considered in the present study as depicted in table 2 aims to find the best possible solutions that strike a balance between multiple objectives rather than focusing on a single objective. The methodology typically consists of the following steps:

1. Problem Formulation, 2. Objective Function Evaluation, 3. Pareto Front

Generation, 4. Solution Space Exploration, 5. Optimization Algorithms 6. Fitness Assessment, 7. Iterative Refinement, 8. Decision Making, 9. Sensitivity Analysis, 10. Result Visualization

Overall, the methodology of multi-objective optimization is a systematic and iterative process that considers multiple objectives and explores the solution space to find a range of optimal solutions. It enables decision-makers to make informed choices by understanding the trade-offs between conflicting objectives and identifying the most favorable solutions based on their preferences.

Table 2: Listing of process and response factors

Class	Designation	Description	Unit	Data range/objective
Factor 1	Independent factors	Radius of the shelling drum	m	$0.0788 < x_1 < 0.212$
Factor 2		Radius of the concave mesh	m	$0.0914 < x_2 < 0.2538$
Factor 3		Surface area in contact with shelling blades	m ²	$0.3028 < x_3 < 0.5452$
Factor 4		Rasp bar spacing	m	$0.01 < x_4 < 0.016$
Factor 5		Number of shelling blades	-	$3 < x_5 < 6$
Response 1	Dependent factor	Mechanical damage	g/sec	Min
Response 1		Shelling efficiency	%	Max
Response 2		Throughput capacity	%	Max

2.4 Computer Aided Design (CAD)

Computer-Aided Design (CAD) using SolidWorks software involves several steps and procedures to create accurate and precise digital models. The detailed procedure for CAD using SolidWorks software is as follows:

1. Requirement Analysis,
 2. Conceptualization,
 3. Creating a New Part:
 4. Sketching,
 5. Adding Dimensions and Constraints,
 6. Extrusion and Revolve,
 7. Adding Features,
 8. Assembly,
 9. Rendering and Visualization,
 14. Revision and Iteration,
 15. Finalization.
- Once the design is complete and meets all the requirements, finalize the CAD project by saving the files in picture format as shown in figures 1 – 3 .

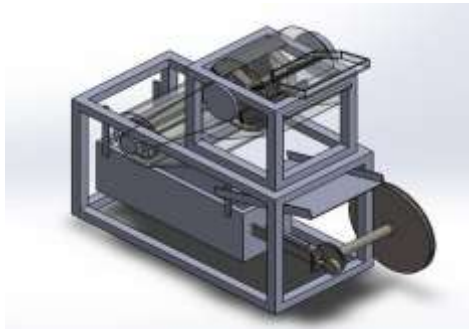


Figure 1 The CAD model of the groundnut shelling machine showing 3D view

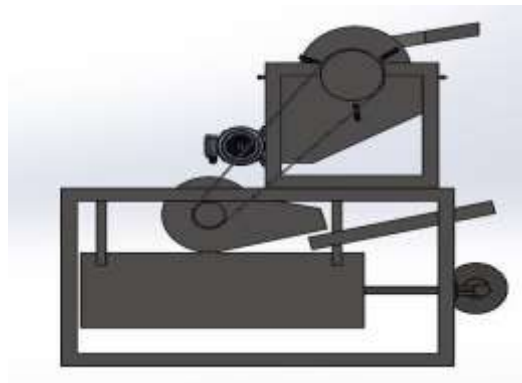


Figure 2 The CAD model of the groundnut shelling machine showing side view



Figure 3: The CAD model of the shelling chamber arrangement

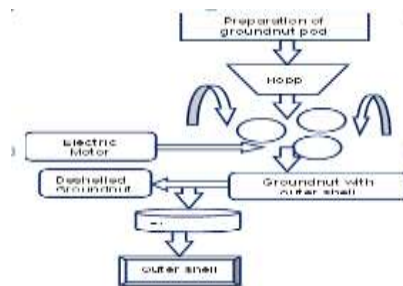


Figure. 4: The flow process of groundnut shelling

2.5 Performance Evaluation

The efficiency is obtained from the relations shown below:

$$\text{Throughput capacity} = \frac{\text{Quantity of groundnut fed}}{\text{Time take}} \quad (5)$$

$$\text{Shelling efficiency} = \frac{\text{weight of groundnut shelled}}{\text{Weight of groundnut fed into machine}} \times 100\% \quad (6)$$

$$\text{Mechanical damage} = \frac{\text{weight of broken seeds}}{\text{Weight of groundnut fed into machine}} \times 100\% \quad (7)$$

Mass of groundnut seeds = 300g

3. RESULTS/DISCUSSION

3.1 Material Selection

In a search for standard materials that might fit the groundnut sheller's in-service condition, it was determined that the following materials, which are shown in Table 3, was utilized for the application. According to Table 3, the goals for each parameter depicted were the strong, light tension members, stiff light tension

members, light stiff beam in deflection, strong light torsion members, and inexpensive stiff support for columns. According to the literature, material with the highest material performance index is typically chosen. The most preferable of the six possible materials is carbon steel, which is followed in preference by low alloy steel, aluminium, wrought iron, stainless steel, and oak wood, as illustrated in table 3.

Table 3. Candidate materials for shelling drum and frame structure

Material	Density (kg/m ³) (ρ)	Price (USD/kg) (C_m)	Yield strength (MPa) (σ_y)	Elastic modulus (MPa) (E)	$\frac{\sigma_f}{\rho}$	$\frac{E}{\rho}$	$\frac{E^{1/2}}{\rho}$	$\frac{E^{1/2}}{C_m \rho}$	Rank
Aluminum	2710	1.55	40	70500	0.0148	26.0148	13.0074	8.3919	3
Carbon steel	7850	0.666	285	210000	0.0363	26.7516	13.3758	20.0838	1
Low alloy steel	7830	1.19	1600	205000	0.2043	26.1814	13.0907	11.0006	2
Wrought iron	7600	0.69	210	190000	0.0276	25.0000	12.5000	18.1159	4
Oak wood	710	2.47	52.5	12800	0.0739	18.0282	9.0141	3.6494	6
Stainless steel	7670	5.18	310	172000	0.0404	22.4250	11.2125	2.1646	5

3.2 Modelling and Performance analysis

The experiments designed for the machine and its impact on mechanical damage, shelling efficiency, and throughput capacity were carried out in a randomized sequence. By conducting these experiments in a randomized sequence, the effect of uncontrolled variables were minimized, ensuring that the observed effects resulted to variations in the independent variables rather than to external or unaccounted factors. The regression equations for mechanical damage (Y1), shelling efficiency (Y2), and throughput capacity (Y3) in uncoded units reflects a comprehensive approach to modeling the shelling process. These equations encapsulate the relationship between the independent variables (X1 to X5) and the response variables (Y1 to Y3), incorporating both linear and nonlinear terms as well as interaction effects. This complexity is indicative of the multifaceted nature of the shelling process, where the

mesh, the surface area in contact with shelling blades, rasp bar spacing, and the number of shelling blades interact in complex ways to influence the outcomes.

The use of the least squares technique to fit these models is a standard and powerful method for dealing with regression analysis, optimizing the parameters of the model to minimize the sum of the squared differences between observed and predicted values.

The normality of errors, a critical assumption in regression analysis, was verified by analyzing the normal probability plot of standardized residuals. This step is essential to confirm that the residuals (differences between observed and predicted values) follow a normal distribution, implying that the model's predictions are unbiased and that the error variance is constant. Statistical software played a crucial role in this comprehensive analysis, enabling the execution of complex calculations, the generation of graphical

representations like Pareto charts and interaction effect plots, and the identification of optimal parameter conditions. These tools not only facilitate a deeper understanding of the data but also enhance the decision-making process by

highlighting their interactions for improved performance. Equations 8 -9 represent the mathematical model developed to predict mechanical damage, shelling efficiency, and throughput capacity, expressed actual parameters.

Regression Equation in Uncoded Units mechanical damage (Y_1)

$$Y_1 = 10.64 + 17.02 X_1 + 15.76 X_2 + 0.97 X_3 - 307 X_4 + 0.426 X_5 - 33.8 X_1 * X_1 - 27.47 X_2 * X_2 + 0.52 X_3 * X_3 + 9040 X_4 * X_4 - 0.0183 X_5 * X_5 + 2.8 X_1 * X_2 + 0.62 X_1 * X_3 - 50 X_1 * X_4 + 0.150 X_1 * X_5 + 0.64 X_2 * X_3 - 46 X_2 * X_4 + 0.113 X_2 * X_5 - 10 X_3 * X_4 + 0.034 X_3 * X_5 - 1.9 X_4 * X_5 \quad (8)$$

Regression Equation in Un-coded Units shelling efficiency (Y_2)

$$Y_2 = 88.77 - 48.4 X_1 - 44.7 X_2 - 0.0 X_3 + 443 X_4 - 1.36 X_5 + 93.3 X_1 * X_1 + 76.0 X_2 * X_2 - 4.0 X_3 * X_3 - 15139 X_4 * X_4 + 0.0578 X_5 * X_5 + 3.0 X_1 * X_2 + 0.6 X_1 * X_3 - 13 X_1 * X_4 + 0.15 X_1 * X_5 + 0.6 X_2 * X_3 - 5 X_2 * X_4 + 0.13 X_2 * X_5 - 0 X_3 * X_4 + 0.03 X_3 * X_5 - 0.6 X_4 * X_5 \quad (9)$$

Regression Equation in Un-coded Units for Throughput capacity (Y_3)

$$Y_3 = 59.98 - 29.86 X_1 + 8.46 X_2 - 0.51 X_3 - 368 X_4 - 2.202 X_5 + 59.3 X_1 * X_1 - 16.79 X_2 * X_2 - 0.90 X_3 * X_3 + 5341 X_4 * X_4 + 0.1275 X_5 * X_5 - 0.5 X_1 * X_2 + 0.3 X_1 * X_3 + 44 X_1 * X_4 + 0.188 X_1 * X_5 - 0.00 X_2 * X_3 - 15 X_2 * X_4 - 0.031 X_2 * X_5 + 3 X_3 * X_4 + 0.021 X_3 * X_5 + 3.9 X_4 * X_5 \quad (26)$$

The significance of the factors was determined by assessing the fitted models using the Fisher's exact test (p -value < 0.05) and confidence intervals based on ANOVA methodology. The suitability of the models was evaluated by examining model adequacy, error independency, and coefficient of determination (R^2) for each variable. The normality of errors was assessed by analysing the normal probability plot of standardized residuals. Statistical software was utilized to obtain the necessary statistical parameters, such as the Pareto chart and interaction effect plots, which aided in identifying the optimal parameter conditions.

3.3 Validation of the model through ANOVA

The ANOVA technique was used to assess the adequacy and significance of each coefficient in the developed model. Table 4-6 presents the standard error of estimated coefficients, multiple correlations, and coefficient of determination (R^2) for all main effects and two-way interactions obtained from the regression analysis. The significance of each effect in the model was determined by the p -value, which indicates the statistical significance according to Montgomery et al. (2008).

Table 4: Analysis of Variance for mechanical damage (Y1)

Source	DF	Adj SS	Adj MS	F-Value	P-Value
Model	20	23.8034	1.19017	13.45	0.000
Linear	5	21.9102	4.38203	49.53	0.000
X1	1	6.7416	6.74160	76.20	0.000
X2	1	7.4371	7.43707	84.07	0.000
X3	1	0.9362	0.93615	10.58	0.008
X4	1	2.1841	2.18407	24.69	0.000
X5	1	4.6113	4.61127	52.12	0.000
Square	5	1.8763	0.37526	4.24	0.021
X1*X1	1	0.6590	0.65900	7.45	0.020
X2*X2	1	0.9624	0.96244	10.88	0.007
X3*X3	1	0.0017	0.00170	0.02	0.892
X4*X4	1	0.1942	0.19419	2.20	0.167
X5*X5	1	0.0496	0.04964	0.56	0.470
2-Way Interaction	10	0.0170	0.00170	0.02	1.000
X1*X2	1	0.0036	0.00360	0.04	0.844
X1*X3	1	0.0004	0.00040	0.00	0.948
X1*X4	1	0.0016	0.00160	0.02	0.895
X1*X5	1	0.0036	0.00360	0.04	0.844
X2*X3	1	0.0006	0.00063	0.01	0.935
X2*X4	1	0.0020	0.00203	0.02	0.882
X2*X5	1	0.0030	0.00302	0.03	0.857
X3*X4	1	0.0002	0.00023	0.00	0.961
X3*X5	1	0.0006	0.00062	0.01	0.935
X4*X5	1	0.0012	0.00123	0.01	0.908
Error	11	0.9731	0.08847		
Lack-of-Fit	6	0.9731	0.16219	*	*
Pure Error	5	0.0000	0.00000		
Total	31	24.7765			

$R\text{-sq} = 96.07\%$, $R\text{-sq}(adj) = 88.93\%$

Table 5: Analysis of Variance for shelling efficiency (Y2)

Source	DF	Adj SS	Adj MS	F-Value	P-Value
Model	20	140.789	7.0394	9.38	0.000
Linear	5	127.456	25.4913	33.97	0.000
X1	1	42.667	42.6667	56.86	0.000
X2	1	46.984	46.9840	62.61	0.000
X3	1	3.345	3.3451	4.46	0.058
X4	1	0.427	0.4267	0.57	0.467
X5	1	34.034	34.0340	45.35	0.000
Square	5	13.318	2.6637	3.55	0.037
X1*X1	1	5.022	5.0215	6.69	0.025
X2*X2	1	7.370	7.3700	9.82	0.010
X3*X3	1	0.101	0.1012	0.13	0.720
X4*X4	1	0.545	0.5445	0.73	0.412
X5*X5	1	0.496	0.4957	0.66	0.434
2-Way Interaction	10	0.014	0.0014	0.00	1.000
X1*X2	1	0.004	0.0042	0.01	0.942
X1*X3	1	0.000	0.0004	0.00	0.982
X1*X4	1	0.000	0.0001	0.00	0.991

X1*X5	1	0.004	0.0036	0.00	0.946
X2*X3	1	0.001	0.0006	0.00	0.977
X2*X4	1	0.000	0.0000	0.00	0.995
X2*X5	1	0.004	0.0042	0.01	0.942
X3*X4	1	0.000	0.0000	0.00	1.000
X3*X5	1	0.000	0.0004	0.00	0.982
X4*X5	1	0.000	0.0001	0.00	0.991
Error	11	8.255	0.7504		
Lack-of-Fit	6	8.255	1.3758	*	*
Pure Error	5	0.000	0.0000		
Total	31	149.043			

$R\text{-sq} = 94.46\%$, $R\text{-sq}(adj) = 84.39\%$

Table 6: Analysis of Variance for Throughput capacity (Y3)

Source	DF	Adj SS	Adj MS	F-Value	P-Value
Model	20	79.7286	3.9864	34.26	0.000
Linear	5	74.8470	14.9694	128.65	0.000
X1	1	13.2313	13.2313	113.71	0.000
X2	1	0.8067	0.8067	6.93	0.023
X3	1	0.4161	0.4161	3.58	0.085
X4	1	9.1761	9.1761	78.86	0.000
X5	1	51.2168	51.2168	440.17	0.000
Square	5	4.8690	0.9738	8.37	0.002
X1*X1	1	2.0300	2.0300	17.45	0.002
X2*X2	1	0.3593	0.3593	3.09	0.107
X3*X3	1	0.0051	0.0051	0.04	0.838
X4*X4	1	0.0678	0.0678	0.58	0.461
X5*X5	1	2.4131	2.4131	20.74	0.001
2-Way Interaction	10	0.0127	0.0013	0.01	1.000
X1*X2	1	0.0001	0.0001	0.00	0.977
X1*X3	1	0.0001	0.0001	0.00	0.977
X1*X4	1	0.0012	0.0012	0.01	0.920
X1*X5	1	0.0056	0.0056	0.05	0.830
X2*X3	1	0.0000	0.0000	0.00	1.000
X2*X4	1	0.0002	0.0002	0.00	0.966
X2*X5	1	0.0002	0.0002	0.00	0.966
X3*X4	1	0.0000	0.0000	0.00	0.989
X3*X5	1	0.0002	0.0002	0.00	0.966
X4*X5	1	0.0049	0.0049	0.04	0.841
Error	11	1.2799	0.1164		
Lack-of-Fit	6	1.2799	0.2133	*	*
Pure Error	5	0.0000	0.0000		
Total	31	81.0085			

$R\text{-sq} = 98.42\%$, $R\text{-sq}(adj) = 95.55\%$

3.4. 3D Plot and Pareto Chart of Standardized Effects

The Pareto chart visually displays the standardized effects in descending order, ranging from the largest to the smallest effect. It also includes a reference line to indicate the statistically significant effects. The impacts of the considered parameters and their interactions on the response are depicted in a Pareto chart, as shown in

Figures 5 to 7. This chart presents the absolute values of the main parameter effects and interaction effects in the form of horizontal bars. A reference line is drawn to identify potentially important factors, with those extending beyond the line considered statistically significant at a 95% confidence level. The Pareto chart provides insights into the relative importance of different factor combinations.

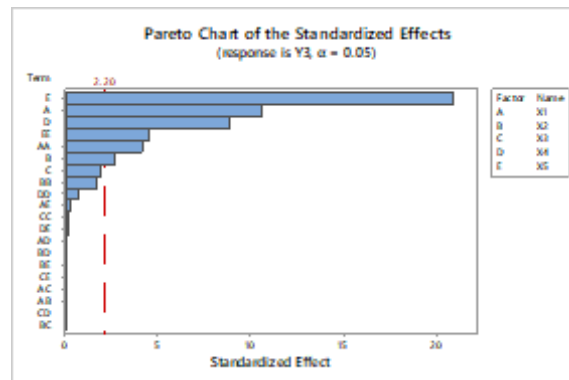


Figure 5: Pareto chart of the standardized effects for throughput capacity (Y3)

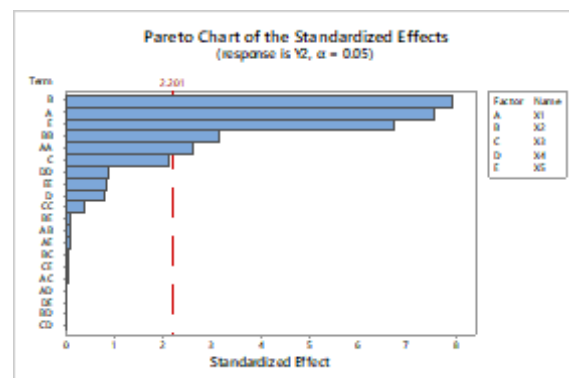


Figure 6: Pareto chart of the standardized effects for Shelling efficiency (Y2)

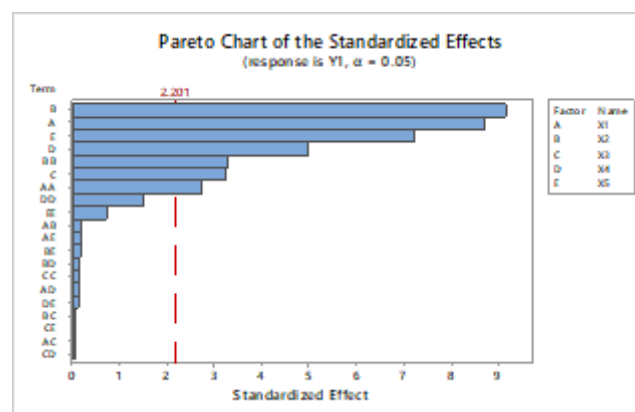


Figure 7. Pareto Chart of the standardized Effects for Mechanical Damage (Y1)

Use 3D Surface Plot to examine the relationship between a response variable (Y3) and two predictor variables X1 and X2 (Figure. 8 - 10) by viewing a three-dimensional surface of the predicted response. The predicted response has been represented as a wireframe. Optimization of the shelling chamber variable parameter was carried out in a numerical optimization

method. The response surface and contour plot at optimum shelling condition for maximum throughput capacity (Y3), Shelling efficiency (Y2) and minimum mechanical damage (Y1). From the results, it was concluded that the developed model could accurately predict the optimum groundnut shelling. The detail of optimization condition is shown in Table 7.

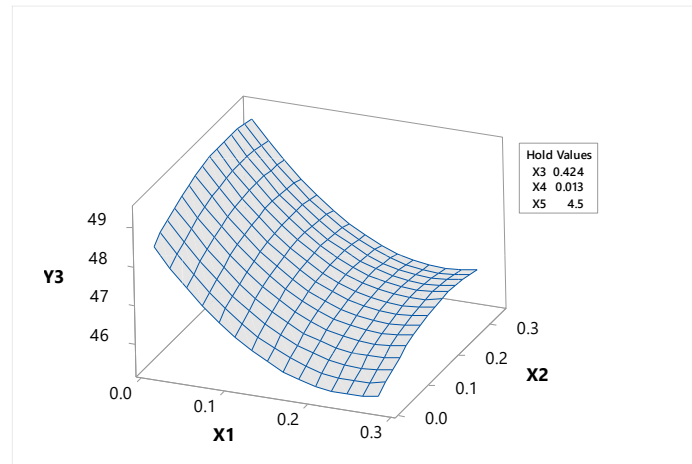


Figure 8: 3D Surface Plot for throughput capacity (Y3)

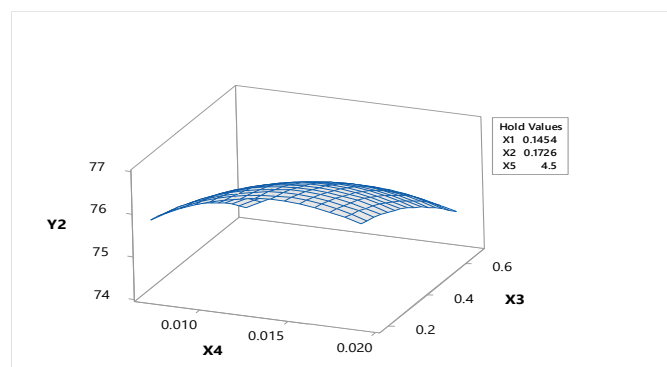


Figure 9: 3D Surface Plot for Shelling efficiency (Y2)

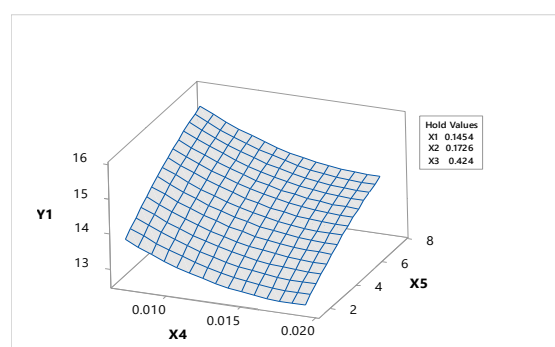


Figure 10: 3D Surface Plot for mechanical damage (Y1)

*Corresponding author, e-mail: engrkekule02@gmail.com, idorenyinmarkson@uniuyo.edu.ng, anaidhuno.ufuoma@fupre.edu.ng, ashiedu.ifeanyi@fupre.edu.ng

3.5 Multiple Response Prediction and Solution

Minitab software utilizes the values provided in the table to compute the fits for all the responses, as depicted in Table 7. The fitted values, represented as "Fit," serve as point estimates of the mean response for specific predictor values. These predictor values are also referred to as x-values. By employing the regression equation and the given variable settings, Minitab calculates the fit. A global optimal condition was

found (X_1) of 0.17, mesh (X_2) of 0.0914, surface area in contact with shelling blades (X_3) of 0.424, rasp bar spacing (X_4) of 0.013 and number of shelling blades (X_5) of 1.5. which was approximated to 3 for safety to conform with stability and balance requirements. At these conditions, mechanical damage (Y_1), shelling efficiency (Y_2), and throughput capacity (Y_3) were 12.32%, 80.4942% and 50.22 g/sec respectively as shown in table 7.

Table 7. Multiple Response Prediction and Solution for Y_3 , Y_2 , Y_1

Response	Fit	SE Fit	95% CI	95% PI					
Y3	50.216	0.328	(49.495, 50.937)	(49.175, 51.257)					
Y2	80.494	0.832	(78.663, 82.325)	(77.851, 83.138)					
Y1	12.323	0.286	(11.694, 12.952)	(11.415, 13.230)					
Solution	X1	X2	X3	X4	X5	Y3 Fit	Y2 Fit	Y1 Fit	Composite Desirability
1	0.17	0.0914	0.424	0.0130606	1.5	50.2163	80.4942	12.3228	0.811831

The determined optimal values were deployed in fabricating the relevant components in the machine, these components were subsequently assembled together using various techniques such as welding, bolting, or fastening. Proper alignment and positioning of the components are critical for effectiveness. Electrical components, such as motors was integrated into the machine to enable its mechanised operation. During the fabrication process, author maintained a focus on precision, accuracy, and adherence to safety standards. The completed machine is pictured in figure 11.

4 CONCLUSIONS

Shelling efficiency, a critical factor in determining effectiveness, was found to be 80%, signifying the machine's success in removing shells from groundnuts, resulting in a high yield of shelled kernels. The throughput capacity, representing the quantity of groundnuts processed within a specific time frame, was determined to be 50 grams per second, indicating the machine's suitability for small to medium-scale groundnut processing. Minimizing kernel damage during shelling is a

significant challenge, and the experimental results demonstrated the groundnut shelling machine's effectiveness in this aspect. The machine achieved a kernel damage rate of

12.5%, indicating that the majority of shelled kernels remained intact and undamaged.



Figure 11: Picture view of the fabricated groundnut shelling machine

REFERENCES

- Adetola O., Akinniyi O., and Olukunle E. (2022). Development and Performance Evaluation of a Groundnut Shelling Machine. *International Journal of Engineering Science and Application*, 6(3), 85-94.
- Ashby M., Cope E., and Cebon D. (2013) Materials selection for engineering design. In *Informatics for materials science and engineering*. Butterworth-Heinemann. pp. 219-244.
- Ashby S.E., Ryan S., Gray M., and James C. (2013) Factors that influence the professional resilience of occupational therapists in mental health practice. *Australian occupational therapy journal*, 60(2), 110-119.
- Cardoso A., Colim A., Bicho E., Braga A.C., Menozzi M., and Arezes P. (2021). Ergonomics and human factors as a requirement to implement safer collaborative robotic workstations: A literature review. *Safety*, 7(4), 71.
- Chang A. S., Sreedharan A., and Schneider K.R. (2013) Peanut and peanut products: A food safety perspective. *Food Control*, 32(1), 296-303.
- Colim A., Faria C., Cunha J., Oliveira J, Sousa N., and. Rocha L.A. (2021) Physical ergonomic improvement and safe design of an assembly workstation through collaborative robotics. *Safety*, 7(1), 14.
- Galea M., Giangrande P., Madonna V. G. (2020) Reliability-oriented design of electrical machines: the design process for machines' insulation systems must evolve. *IEEE Industrial Electronics Magazine*, 14(1), 20-28.
- Gauthier F., Chinniah Y., Abdul-Nour G., Jocelyn S., Aucourt B., Bordeleau G., and. Mosbah, A.B. (2021). Practices and needs of machinery designers and manufacturers in

- safety of machinery: An exploratory study in the province of Quebec, Canada. *Safety Science*, 133, 105011.
- Gupta K., and Gupta M.K. (2020) Optimization of Manufacturing Processes. Springer International Publishing.
- Hoque M.A, Hossain M. Z., and Hossain M.A. (2018) Design and development of a power groundnut sheller. *Bangladesh Journal of Agricultural Research*, 43(4), 631-645.
- Hua Y., Liu Q., Hao K., and Jin Y. (2021). A survey of evolutionary algorithms for multi-objective optimization problems with irregular Pareto fronts. *IEEE/CAA Journal of Automatica Sinica*, 8(2), 303-318.
- Iqbal Z., Jowowasito G., Lutfi M., Wardani F.I., Lubis R. A. Siahaan L. B, and Hidayah I. (2019). Designing small-medium scale groundnut (*Arachis hypogaea* L.) shelling machine for local merchant in Tuban, East Java. In *IOP Conference Series: Earth and Environmental Science* (Vol. 230, No. 1, p. 01 2013. IOP Publishing.
- Meneely J.P., Kolawole O., Haughey S. A., Miller S. J., Krska R., and Elliott C. T. (2022) The challenge of global aflatoxins legislation with a focus on peanuts and peanut products: a systematic review. *Exposure and Health*, 1-21.
- Montgomery M.R, (2008) The urban transformation of the developing world. *science*, 319(5864), 761-764.
- Muhammad A.I, and Isiaka M. (2019) Modification of locally developed groundnut sheller. *Bayero Journal of Engineering and Technology*, 14(2), 169-182.
- Ravindra A., Rohit G., Saurav A., and Khare G.N. (2017) A review on design and fabrication of groundnut shelling and separating machine. *International Research Journal of Engineering and Technology*, 4(10), 1403-1406.
- Sasikumar A., Turon A., Cózar I.R., Vallmajó O., Casero J.C., De Lozzo M., and Abdel-Monsef S. (2023). Sensitivity analysis methodology to identify the critical material properties that affect the open hole strength of composites. *Journal of Composite Materials*, 57(10), 1791-1805.
- Sharifi M.R., Akbarifard S., Qaderi K., and Madadi M.R. (2021). A new optimization algorithm to solve multi-objective problems. *Scientific Reports*, 11(1), 20326.
- Sun Q., Wang C., Wang Z., Zhao Y., and Bao C. (2017) Design and Experiment of a Peanut Shelling Machine. *Agricultural Research*, 6, 304-311.
- Wangette I. S., Nyaanga D.M., and Njue M. R. (2015) Influence of groundnut and machine characteristics on motorised sheller performance. *American Journal of Agriculture and Forestry*, 3(5), 178-191.
- Yazdani M., Zavadskas E.K, Ignatius J. and Abad M.D. (2016) Sensitivity analysis in MADM methods: Application of material selection. *Engineering Economics*, 27(4), 382-391.